

Photoaffinity Labeling the Propofol Binding Site in GLIC

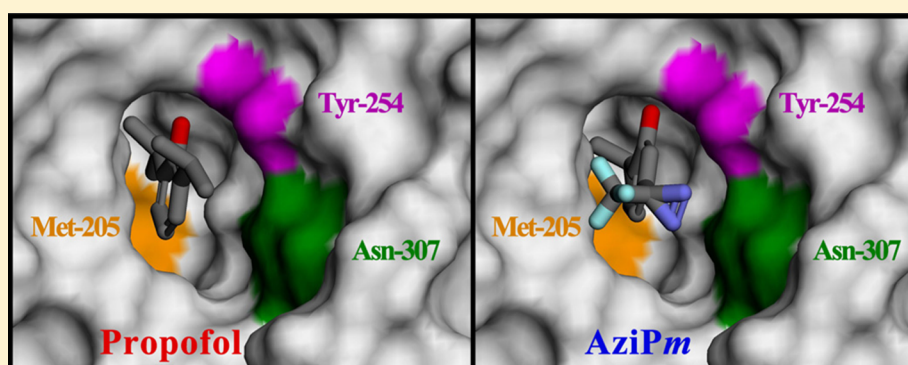
David C. Chiara,[†] Jonathan F. Gill,[†] Qiang Chen,[‡] Tommy Tillman,[‡] William P. Dailey,[§] Roderic G. Eckenhoff,[§] Yan Xu,[‡] Pei Tang,^{*,‡} and Jonathan B. Cohen^{*,†}

[†]Department of Neurobiology, Harvard Medical School, Boston, Massachusetts 02115, United States

[‡]Department of Anesthesiology, University of Pittsburgh School of Medicine, Pittsburgh, Pennsylvania 15260, United States

[§]Department of Anesthesiology and Critical Care, Perelman School of Medicine, University of Pennsylvania, Philadelphia, Pennsylvania 19104, United States

S Supporting Information



ABSTRACT: Propofol, an intravenous general anesthetic, produces many of its anesthetic effects in vivo by potentiating the responses of GABA type A receptors (GABA_AR), members of the superfamily of pentameric ligand-gated ion channels (pLGICs) that contain anion-selective channels. Propofol also inhibits pLGICs containing cation-selective channels, including nicotinic acetylcholine receptors and GLIC, a prokaryotic proton-gated homologue from *Gloeobacter violaceus*. In the structure of GLIC cocrystallized with propofol at pH 4 (presumed open/desensitized states), propofol was localized to an intrasubunit pocket at the extracellular end of the transmembrane domain within the bundle of transmembrane α -helices (Nury, H, et al. (2011) *Nature* 469, 428–431). To identify propofol binding sites in GLIC in solution, we used a recently developed photoreactive propofol analogue (2-isopropyl-5-[3-(trifluoromethyl)-3H-diazirin-3-yl]phenol or AziPm) that acts as an anesthetic in vivo and potentiates GABA_AR in vitro. For GLIC expressed in *Xenopus* oocytes, propofol and AziPm inhibited current responses at pH 5.5 (EC₂₀) with IC₅₀ values of 20 and 50 μ M, respectively. When [³H]AziPm (7 μ M) was used to photolabel detergent-solubilized, affinity-purified GLIC at pH 4.4, protein microsequencing identified propofol-inhibitable photolabeling of three residues in the GLIC transmembrane domain: Met-205, Tyr-254, and Asn-307 in the M1, M3, and M4 transmembrane helices, respectively. Thus, for GLIC in solution, propofol and AziPm bind competitively to a site in proximity to these residues, which, in the GLIC crystal structure, are in contact with the propofol bound in the intrasubunit pocket.

The primary target for many general anesthetics including propofol is the γ -aminobutyric acid type-A receptor (GABA_AR), the main inhibitory receptor in the brain.^{1–3} Propofol potentiates GABA_AR responses at anesthetic concentrations, whereas at higher concentrations it inhibits other members of the pentameric ligand-gated ion channel (pLGIC) superfamily that contain cation-selective channels, including nicotinic acetylcholine receptors (nAChR)^{4–6} and the prokaryotic pLGIC from *Gloeobacter violaceus* (GLIC), a proton-gated ion channel.⁷ Identification of propofol binding sites in pLGICs is necessary to determine whether it binds to equivalent or distinct sites when it acts as a positive or a negative allosteric pLGIC modulator. Each pLGIC subunit is composed of an N-terminal extracellular domain, composed of primarily β strands, and a transmembrane domain consisting of

a loose bundle of four α -helices, designated M1–M4.^{8,9} When five subunits assemble to form a pLGIC, the M2 helices from each subunit combine to line the ion channel and are protected from the lipid by the M1, M3, and M4 helices.

Crystal structures of a GABA_AR are not as yet available. However, several structures of prokaryotic pLGICs homologous with the GABA_AR have been solved with general anesthetics bound, including GLIC with an intrasubunit binding site in the transmembrane domain (TMD) for propofol (or desflurane)¹⁰ and an intersubunit site for bromoform¹¹ as well as a binding site for ketamine in the extracellular domain.¹²

Received: November 5, 2013

Revised: December 13, 2013

Published: December 16, 2013



In ELIC, a pLGIC from *Erwinia chrysanthemi*, binding sites were identified for bromoform in the TMD in the ion channel, at an interface between adjacent subunits, and in the extracellular domain.¹³ When propofol was cocrystallized with GLIC, propofol bound to a site near the extracellular end of the TMD in a pocket formed by the four transmembrane helices, and site-directed mutations of residues lining this intrasubunit pocket affected the inhibitory action of propofol.¹⁰ In contrast, in GLIC expressed in *Xenopus* oocytes, a substituted Cys within this intrasubunit pocket was more susceptible to modification in the presence of propofol, whereas a substituted Cys at a position predicted to be in a pocket between helices of adjacent subunits (an intersubunit pocket) was protected from modification by propofol,¹⁴ which suggests that propofol binds to pockets between adjacent subunits.

Photoaffinity labeling allows the identification of amino acids in a protein that contribute to a drug binding site without any assumptions about the points of drug contact in a protein (reviewed in ref 15), and photoreactive analogues of etomidate and mephobarbital have been used recently to identify two classes of intersubunit general anesthetic binding sites in the GABA_AR transmembrane domain.^{16–18} A photoreactive propofol analogue, 2-isopropyl-5-[3-(trifluoromethyl)-3H-diazirin-3-yl]phenol or AziPm, was developed recently that acts as an anesthetic in vivo and potentiates GABA_AR responses in vitro.¹⁹ AziPm, which contains a photoreactive trifluoromethyl diazirine that can react with most amino acid side chains, also is a *Torpedo* (muscle-type) nicotinic acetylcholine receptor (nAChR) negative allosteric modulator.²⁰ In the *Torpedo* nAChR in native membranes, there is propofol-inhibitable photolabeling by [³H]AziPm of amino acids in binding sites in (i) the ion channel and (ii) in the δ subunit helix-bundle pocket, a pocket homologous to the propofol binding site identified in GLIC crystals.²⁰ [³H]AziPm also photolabeled an amino acid in the transmembrane domain in the pocket between the γ and α subunits, but that photolabeling was enhanced rather than inhibited by propofol. In this work, we demonstrate that AziPm inhibits GLIC currents in oocytes with an IC₅₀ and Hill coefficient similar to propofol. Photolabeling detergent-solubilized, affinity-purified GLIC with [³H]AziPm at pH 4.4, a pH that stabilizes the open or desensitized state,²¹ identified propofol-inhibitable labeling of residues in M1, M3, and M4, consistent with both AziPm and propofol occupying the propofol binding site identified by X-ray crystallography.

EXPERIMENTAL PROCEDURES

Materials. Milligram quantities of GLIC were obtained by expression in *Escherichia coli*, detergent solubilization, and affinity purification, as described.²² Purified GLIC was stored at 3 °C in 10 mM K₂HPO₄/KH₂PO₄ (pH 8.0), 150 mM NaCl, and 0.075% dodecyl maltoside. Nonradioactive 2-isopropyl-5-[3-(trifluoromethyl)-3H-diazirin-3-yl]phenol (AziPm) was synthesized as described,¹⁹ and [³H]AziPm (10 Ci/mmol) was prepared by custom tritiation at AmBios (Newington, CT). Propofol and 3-bromo-3-methyl-2-(2-nitrophenylthio)-3H-indole (BNPS-skatole) were from Sigma, *o*-phthalaldehyde (OPA) was from Alfa Aesar, and *Lysobacter enzymogenes* endoprotease Lys-C (EndoLys-C) was from Roche Applied Science.

Two-Electrode Voltage Clamp. Capped complementary RNA expressing GLIC was synthesized with the mMessage mMachine SP6 kit (Ambion) and purified with the RNeasy kit (Qiagen), and 25 ng was injected into *Xenopus laevis* stage 5 to

6 oocytes. Oocytes were maintained at 18 °C in modified Barth's saline. Two-electrode voltage-clamp experiments were performed at room temperature 16–48 h after injection with a model OC-725C amplifier (Warner Instruments) and a 20 μ L oocyte recording chamber (Automate Scientific). Oocytes were clamped to a holding potential of –60 mV. Currents were recorded in ND-96 supplemented with 10 mM MES and adjusted to the indicated pH. Propofol and AziPm were added at the concentrations indicated. Data were collected and processed using Clampex 10 (Molecular Devices). The currents were normalized to the current measured without drug, and the data were fit to the equation

$$f(x) = 1/(1 + (x/IC_{50})^n)$$

where $f(x)$ is the fraction of current remaining at drug concentration x , IC₅₀ is the drug concentration at which 50% inhibition occurs, and n is the Hill coefficient.

Photoaffinity Labeling of GLIC with [³H]AziPm. Affinity-purified GLIC (400 μ g in 2.3 mL of 10 mM K₂HPO₄/KH₂PO₄ (pH 8.0), 150 mM NaCl, and 0.075% DDM) was adjusted to pH 4.4 by slow titration and gentle vortexing with 550 μ L of 250 mM NaOAc (pH 4), and [³H]AziPm (10 Ci/mmol) was added to 7 μ M. The sample was divided, and 300 μ M propofol was added to half of the sample, resulting in a final GLIC concentration of 0.14 mg protein/mL (i.e., \sim 4 μ M binding sites for a ligand binding to a single site in each subunit). After 30 min on ice, samples were irradiated at 365 nm for 30 min and denatured in sample buffer, and the GLIC subunit was resolved by SDS-PAGE. The Coomassie blue-stained band of GLIC at \sim 37 kDa was excised and eluted for 5 days in 100 mM NH₄HCO₃, 2.5 mM dithiothreitol, and 0.2% SDS, pH 8.4, at 20 °C with gentle agitation. The eluates containing the labeled GLIC protein were filtered, concentrated, acetone precipitated, and resuspended in 100 μ L of 15 mM Tris and 0.1% SDS, pH 8.5.

Enzymatic/Chemical Digestion, Reversed-Phase HPLC, and Automated Edman Degradation. Aliquots of GLIC were digested with 1.5 U of EndoLys-C for 3 weeks at 20 °C. Additional aliquots were loaded directly onto PVDF filters for BNPS-skatole chemical cleavage as described.^{17,23} Reversed-phase HPLC was performed on an Agilent 1100 series HPLC. Separations were achieved at 40 °C on a Brownlee Aquapore Bu-300 7 μ M 100 mm column with aqueous solvent 0.08% trifluoroacetic acid, organic solvent 60% acetonitrile, 40% isopropanol, and 0.05% trifluoroacetic acid, and a gradient beginning at 5% organic and reaching 100% organic in 75 min. Flow rate was 0.2 mL/min, and fractions were collected every 2.5 min. Sequence analysis was performed on a Procise 492 (ABI) protein sequencer using ²/₃ of each cycle for amino acid detection and ¹/₃ for ³H counting (measured ³H and picomole data are shown in the ³H-release plots). Digests were loaded onto Prosorb (ABI) PVDF membranes for sequencing. To isolate chemically specific peptides during sequence analysis, the sequencer was paused prior to an expected proline, and the filter was treated with *o*-phthalaldehyde (OPA) before proceeding. OPA covalently blocks Edman degradation at all free amino-termini residues except prolines.^{24,25}

Modeling and Computational Docking. The CHARMM-based molecular dynamics simulated annealing program CDOCKER (Accelrys Discovery Studio) was used to dock propofol or AziPm into the propofol pocket in one subunit (C) of the GLIC crystal structure (PDB: 3P50). A binding-site sphere (10 Å radius) was centered on the propofol

molecule of the PDB structure, and then all nonprotein molecules were removed from the structure. Beginning with 13 (propofol) or 26 (AziPm) randomly oriented molecules, each of which had 35 random computer reorientations and 35 MD-driven molecular alterations (i.e., 1225 starting points for each), the 100 lowest-energy solutions for each starting molecule were collected (1300 solutions for propofol and 2600 for AziPm).

To compare GLIC and nAChR photolabeling results, a homology model of the *Torpedo californica* nAChR based on the GLIC structure (PDB: 3P50) was made using Discovery Studio. To align the TMD sequences of GLIC and *Torpedo* nAChR subunits, a secondary/tertiary structural alignment was made between GLIC and neuronal $\beta 2$ nAChR TMD NMR structure (PDB: 2LM2)²⁶ using the Superimpose Proteins function, and the resulting sequence alignment was combined with a sequence alignment between *Torpedo* nAChR subunit TMD sequences and neuronal $\beta 2$ nAChR TMD, which share >50% identity. The final TMD alignment between GLIC and *Torpedo* nAChR subunits necessitated one residue insertions in the M1–M2 (δ Pro-250) and M2–M3 (δ Leu-283) loops. The level of the intrasubunit helix-bundle pocket and the composition of the M2–M3 loop in this GLIC-based model differ from that of the CryoEM-based model of nAChR (PDB: 2BG9)⁸ that was used previously to locate the amino acids photolabeled by nAChR inhibitors.^{20,27–29} In the GLIC-based structure, the photolabeled amino acids contribute to a better-defined common binding site situated among the M1, M2, and M3 helices. Comparison of the structures of the two models of the nAChR δ subunit transmembrane domain, including the locations of photolabeled amino acids, are shown in stereo representation in the Supporting Information, Figures S1 and S2 and in Table S1.

RESULTS

Propofol and AziPm Inhibit GLIC. GLIC expressed in *Xenopus* was activated by a decrease in pH from 7.4 to 5.5 for ~20 s, a shift in pH that produced ~20% of the maximal current response elicited by a shift to pH 3.5. Coapplication of propofol with the decrease in pH produced a concentration-dependent inhibition of current responses with an IC_{50} of $21.4 \pm 1.2 \mu M$ and a Hill coefficient of 0.67 ± 0.05 (Figure 1). Similarly, coapplication of AziPm with the decrease in pH inhibited GLIC currents with an IC_{50} of $51.4 \pm 5.3 \mu M$ and a Hill coefficient of 0.63 ± 0.11 .

Characterization of [³H]AziPm Photolabeling of GLIC. Affinity-purified GLIC in detergent solution was equilibrated with [³H]AziPm (7 μM) for 30 min on ice at pH 4.4 in the absence or presence of 300 μM propofol. After irradiation for 30 min at 365 nm, [³H]AziPm-labeled GLIC subunit was isolated by SDS-PAGE. Sequence analysis of the intact subunit revealed the presence of three N-terminal residues (GPM) before the published sequence (GPMGQDM...). (In this article, we use the numbering of amino acids in the GLIC primary structure that is used in the GLIC crystal structure,¹⁰ with the first three residues (GPM) in our subunit omitted.) No ³H-labeled residues were encountered in the first 20 cycles of Edman degradation, and ³H appeared to be stably incorporated in GLIC.

To characterize initially regions of [³H]AziPm photo-incorporation, photolabeled GLIC was digested with EndoLys-C, which cleaves after Lys residues and is predicted to fractionate GLIC into 11 peptides, three of which contain the four hydrophobic transmembrane helices, M1–M4 (Figure

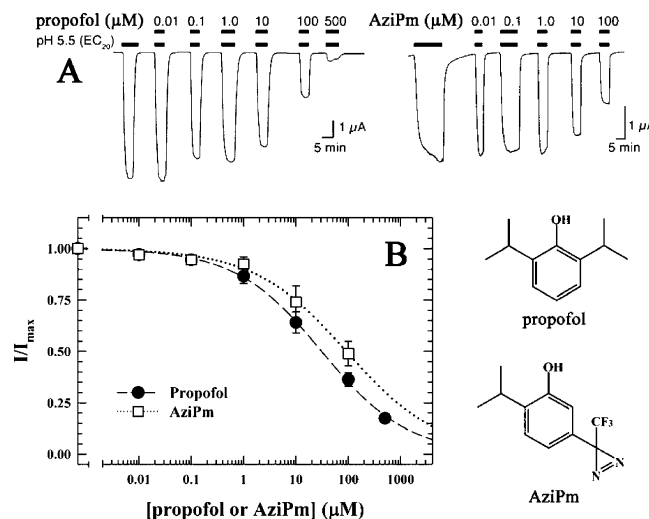


Figure 1. Propofol and AziPm both inhibit H^+ -activated GLIC currents. (A) Representative current traces of oocyte-expressed GLIC exposed to pH 5.5, corresponding to the EC_{20} in the presence of various concentrations of propofol or AziPm, as indicated with black bars over the traces. Limited solubility of AziPm prevented analysis at higher concentrations. (B) Inhibition curves for propofol and AziPm at the pH corresponding to the EC_{20} (pH 5.5). Response is expressed as the fraction of current induced in the presence of the indicated concentrations of propofol (●) or AziPm (□) relative to that in their absence. The data ($n = 7$) were fit to Hill equations with IC_{50} values of 21.4 ± 1.2 and $51.4 \pm 5.3 \mu M$, respectively, and had Hill coefficients of 0.67 ± 0.05 and 0.63 ± 0.11 , respectively. Error bars represent SEM. Also included are the chemical structures of propofol and AziPm.

2A). When the digests were fractionated by reversed-phase HPLC, 80% of the recovered ³H eluted at >60% organic (Figure 2B), and sequence analysis of those fractions identified only the three peptides containing the transmembrane segments (Figure 2C). An additional 15% of ³H eluted in a hydrophilic peak that contained an 84 amino acid GLIC fragment beginning at Thr-65. Therefore, the majority of [³H]AziPm labeling was limited to the transmembrane region of GLIC.

Identification of Propofol-Inhibitable Labeling in M3, M4, and M11. In the amino acid sequence of the GLIC fragment produced by EndoLys-C that begins at Leu-184 and contains the M1 and M2 helices, Pro-199, located near the N-terminus of M1, would occur in the 16th cycle of Edman degradation, whereas the fragments containing M3 and M4 contain prolines in cycles two (Pro-250) and five (Pro-285), respectively. This allowed us to characterize [³H]AziPm photoincorporation in each of the fragments by sequencing aliquots of the total digests and chemically isolating the fragment of interest by treatment of the sample at the cycle of Edman degradation containing the proline of interest with *o*-phthalaldehyde (OPA), which blocks the N-terminus of all peptides not containing a Pro in that cycle.^{24,25}

For analysis of [³H]AziPm photolabeling in M3, sequencing samples were treated with OPA before cycle two (Figure 3A). After the OPA treatment, the only two fragments detected were the fragment beginning at Thr-249 and the N-terminal peptide (which also contains a Pro in cycle two). Because sequence analysis of intact [³H]AziPm-labeled GLIC did not identify any peaks of ³H release in 20 cycles of Edman degradation, the peak of ³H release in cycle six indicated photolabeling of Tyr-254 (115 cpm/pmol), which was inhibited ~80% by 300 μM

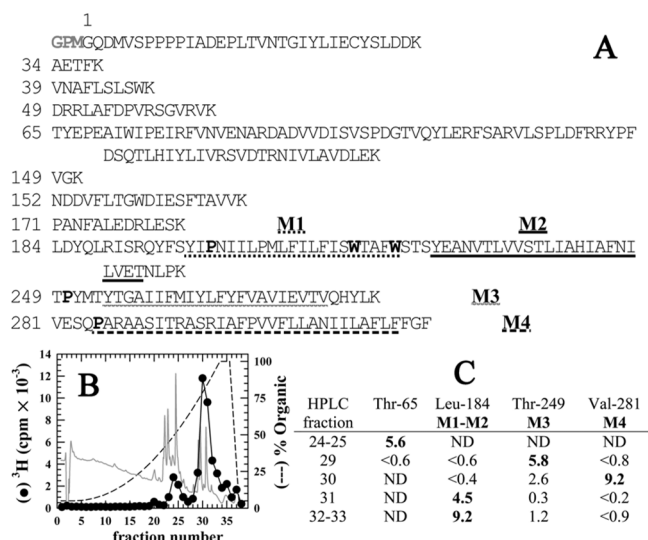


Figure 2. Reversed-phase HPLC fractionation of EndoLys-C digests of GLIC: [^3H]AziPm primarily photoincorporates into the hydrophobic, transmembrane domain of GLIC. (A) Sequences of the GLIC fragments produced by enzymatic cleavage with EndoLys-C (specific for Lys). The residue numbering is that used in the crystal structure (PDB: 3P50¹⁰) and does not include the three additional N-terminal residues (GPM) identified by sequence analysis of intact, expressed GLIC. The transmembrane helices M1–M4 are underlined. The Pro residues used to chemically isolate M1, M3, and M4 during sequencing are in bold as well as the Trp residues subjected to chemical cleavage to sequence M2. (B) Reversed-phase HPLC fractionation of an EndoLys-C digest of [^3H]AziPm labeled GLIC. Eighty-two percent of the recovered ^3H eluted in hydrophobic fractions (>75% organic, fractions 28–38). In gray is the absorbance profile at 215 nm. (C) Selected fractions containing ^3H were sequenced, with the peptides detected quantitated in picomoles. In fractions 29–33, the only GLIC fragments detected were those containing the transmembrane helices. ND, not detected.

propofol. The minor peaks of ^3H release in cycles 13, 15, and 18 indicated that there may also be propofol-insensitive photolabeling in M3 of Met-261, Tyr-263, and Tyr-266 at <20% of the level of labeling of Tyr-254.

For analysis of photolabeling in M4, sequencing samples were treated with OPA before cycle five (Figure 3B). After the OPA treatment, the primary sequence began at Val-281 before M4, and the peak of ^3H in cycle 27 indicated labeling of Asn-307 (300 cpm/pmol) within the M4 helix, which propofol inhibited by 70%. (After treatment with OPA in cycle five, there was also a secondary sequence of the Thr-65 fragment that contains Pro-68 in cycle four that was present at low level in cycle five because of the finite repetitive yield of Edman degradation. The ^3H release in cycle 27 was not associated with Val-90 from this peptide because no ^3H release was detected in cycle 26 when the digest was sequenced without OPA (data not shown).) For analysis of photolabeling in M1, sequencing samples were treated with OPA before cycle 16 (Figure 3C). After the OPA treatment, the only sequence detected originally began at Leu-184. Release of ^3H in cycle 22 indicated photolabeling of Met-205 (41 cpm/pmol) in M1, which propofol inhibited by ~40%.

[^3H]AziPm Photolabeling within M2. To characterize photoincorporation in M2, we took advantage of the distribution of Trp residues within the GLIC primary structure and the ability of BNPS-skatole to cleave peptide bonds C-

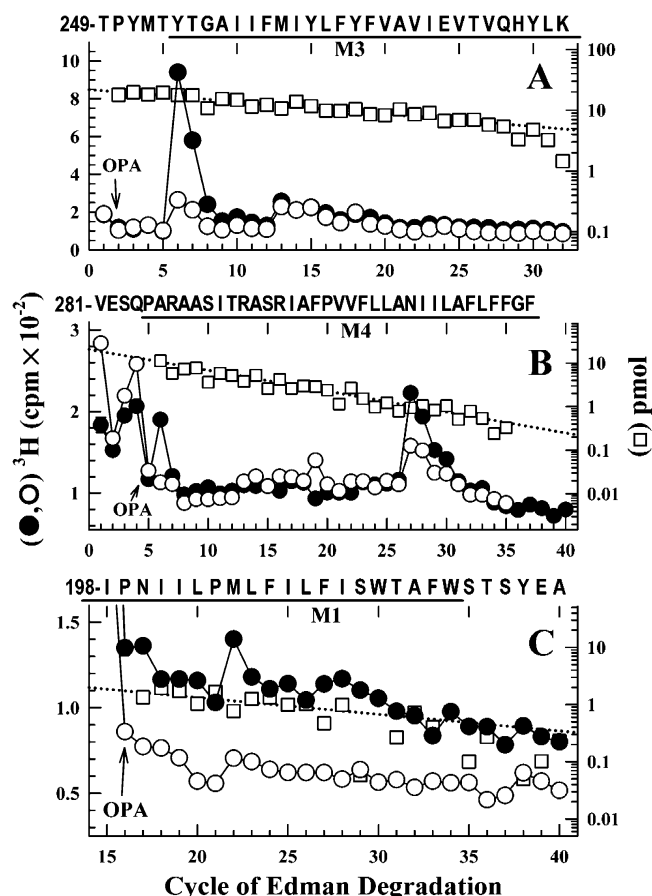


Figure 3. Propofol-inhibitable [^3H]AziPm labeling identified in M3, M4, and M1. ^3H (●, ○) and PTH-amino acids (□) released when equal aliquots of EndoLys-C digests of GLIC photolabeled with [^3H]AziPm in the absence (●) or presence (○, □) of 300 μM propofol were sequenced with OPA treatment in cycles 2 (A), 5 (B), or 16 (C). (A) After OPA treatment in cycle two, the primary sequence began at Thr-249 before M3 ($I_0 = 20$ pmol, both conditions). The GLIC amino-terminal fragment, the only other peptide from an EndoLys-C digest of GLIC with a proline in cycle two, was present (11 pmol, both conditions). The peak of ^3H release in cycle six indicated photolabeling of Tyr-254 at an efficiency of 115 cpm/pmol, which 300 μM propofol inhibited by 83%. The small peak of ^3H release in cycle 13 indicated propofol-insensitive photolabeling of Met-261 at ~20 cpm/pmol. (B) After OPA treatment in cycle five, the primary sequence began at Val-281 before M4 (–PPF, $I_0 = 15$ pmol; +PPF (□), $I_0 = 21$ pmol). The only other peptide present was lag from the fragment beginning at Thr-65 (13 pmol), which contains Pro-68 in cycle four that would also be present in cycle five as a consequence of the ~90% repetitive yield of Edman degradation. The peak of ^3H release in cycle 27 indicated photolabeling of Asn-307 in M4 at 300 cpm/pmol, which 300 μM propofol inhibited by 70%. Because treatment with OPA blocks ~90% of the free amino termini of peptides not containing a Pro, the peak of ^3H release in cycle six after the OPA treatment is consistent with photolabeling of Tyr-254 if the M3 fragment beginning Thr-249 is present at ~7% of the level seen in panel A. (C) After OPA treatment in cycle 16, the primary sequence detected originally began at Leu-184 (–PPF, $I_0 = 9$ pmol; +PPF (□) $I_0 = 5$ pmol). The peak of ^3H release in cycle 22 indicated photolabeling of Met-205 at ~40 cpm/pmol, which propofol inhibited by ~40%.

terminal to tryptophan selectively, producing fragments with free amino termini susceptible to Edman degradation.^{23,17} Of the five Trp residues in GLIC (residues 47, 72, 160, 213, and

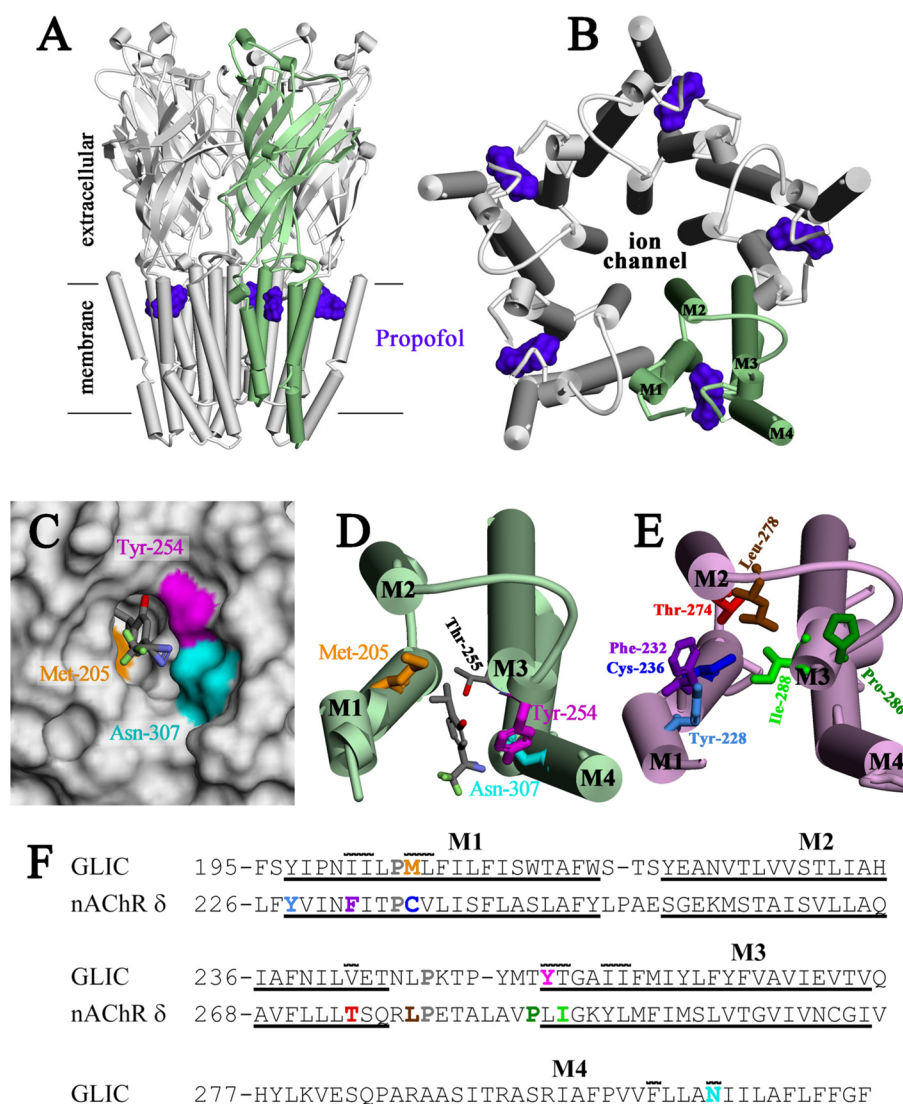


Figure 4. Location of [^3H]AziPm-photolabeled residues in the propofol binding site in GLIC and in the equivalent binding site in the *Torpedo* nAChR δ subunit. (A–D) Views of the crystallographic model of GLIC cocrystallized with propofol (PDB: 3P50). (E) View of the nAChR δ subunit transmembrane domain (TMD) from an nAChR homology model derived from the GLIC structure (see the Experimental Procedures and Supporting Information Figures S1 and S2). α -Helices are shown as cylinders, and β -sheets, as ribbons. (A) View of GLIC from the side and (B) view of the GLIC TMD from the base of the extracellular domain, with one subunit colored green. The positions of propofol within the structure are shown as Connolly surfaces (purple). (C) Connolly surface representation of the propofol binding pocket, viewed from the lipid, with the surfaces contributed by the photolabeled residues color-coded: Tyr-254 (magenta), Asn-307 (cyan), and Met-205 (gold). The lowest-energy docking solution for AziPm is included in stick format, color-coded by atom type: gray, carbon; red, oxygen; blue, nitrogen; light green, fluorine. (D) View of a single subunit's TMD from the same perspective as in panel B, illustrating the position of the docked AziPm solution and the [^3H]AziPm-photolabeled residues in stick format, color-coded as in panel C. The propofol/AziPm binding pocket resides between the M1, M3, and M4 helices. (E) View of the nAChR δ subunit TMD, oriented similar to GLIC in panel D. Residues in the δ subunit helix-bundle pocket photolabeled by various photoreactive nAChR inhibitors are shown in stick format: [^3H]AziPm Phe-232, Cys-236, and Thr-274;²⁰ [^{14}C]halothane δ Tyr-228;³³ [^{125}I]TID Ile-288, Phe-232, Cys-236, Thr-274, and Leu-278;^{27,34,35} [^3H]benzophenone Pro-286, Ile-288, and Phe-232;²⁸ [^3H]azietomidate Cys-232;⁴¹ and [^3H]TFD-etomidate Phe-232 and Cys-236.²⁹ In contrast to the propofol/AziPm site in GLIC, the drug binding pocket in the nAChR δ subunit resides between the M1, M2, and M3 helices. (F) Subunit primary-structure alignment in the M1–M3 region used to make the nAChR homology model from the GLIC structure. The conserved prolines in all pLGICs are shown in gray. Also included is the M4 sequence from GLIC. The extent of the transmembrane helices is denoted by underlining. Photolabeled residues in GLIC and the *Torpedo* nAChR δ subunit are color-coded as in panels D and E. Residues in GLIC in contact with propofol in the crystal structure¹⁰ have a line over them, illustrating the similarities between the intrasubunit pockets of GLIC and *Torpedo* nAChR δ subunit.

217), only Trp-213 and Trp-217 are in the transmembrane region, near the end of the M1 helix (Figure 2A). When photolabeled GLIC was sequenced for 30 cycles after treatment with BNPS-skatole, all six expected peptides were identified, with the fragment beginning at Ser-218 before M2 present at ~ 10 pmol. Any photolabeling of residues in M2, if it occurred,

was at $<10\%$ of the efficiency of photolabeling of Asn-307 in M4 and was insensitive to propofol.

AziPm Docking to the Propofol Binding Site in GLIC. Propofol docking to one of the propofol binding sites in GLIC produced 1300 lowest-energy solutions, each reproducing the orientation of propofol in the PDB structure and differing only

by rotations of $<50^\circ$ of the external isopropyl group. CDocker interaction energies between GLIC and the propofol ranged between -24.7 and -26.3 kcal/mol. For AziPm docking to the same propofol binding site, 2600 lowest-energy solutions were collected with CDocker interaction energies between -24.5 and -26.3 kcal/mol. For all solutions, the diazine nitrogens were positioned between the M1 and M4 helices, oriented toward lipid. In the lowest-energy orientation, depicted in Figure 4C,D and repeated in 2212 of 2600 solutions, the diazine nitrogens were within ~ 3 Å of the hydroxyl of photolabeled Tyr-254 in M3 and the side-chain amide nitrogen of photolabeled Asn-307 in M4. The hydroxyl oxygen of AziPm was 3.4 Å from the hydroxyl of Thr-255 (Figure 4D), suggestive of a hydrogen bond as postulated by Nury et al. for desflurane.¹⁰

DISCUSSION

In this study we used AziPm, a photoreactive analogue of propofol that inhibits pH-gated GLIC responses with a potency similar to that of propofol, to identify AziPm and propofol binding sites in GLIC in detergent solution. When GLIC was photolabeled with [^3H]AziPm at pH 4.4, a condition that stabilizes open or desensitized states,^{30,31} we identified propofol-inhibitable photolabeling of three GLIC residues: Tyr-254 in M3, Asn-307 in M4, and Met-205 in M1. In the structure of GLIC cocrystallized with propofol (Figure 4A–D), these three residues line the propofol binding pocket, with Tyr-254 (M3) and Asn-307 (M4) in contact with each other. AziPm docks to this same pocket (Figure 4C,D) with similar interaction energies as propofol and in a preferred orientation with the diazine ~ 3 Å from Tyr-254 and Asn-307, the most prominently photolabeled residues. Thus, our photolabeling results establish that AziPm and propofol bind to GLIC in solution at pH 4.4 at the same site that propofol binds in the crystal structure. When in the native homopentameric form, GLIC has potentially five equivalent binding sites for propofol or AziPm. In a recent study,³² we used molecular dynamics simulations to compare the conformational transitions of GLIC under various states of propofol occupancy of these equivalent sites. The work concluded that asymmetric binding underlies the propofol functional inhibition of GLIC.

When [^3H]AziPm was used to photolabel another pLGIC, the *Torpedo* nAChR in native membranes,²⁰ propofol-inhibitable labeling was identified of amino acids contributing to two distinct binding sites in the TMD: (i) a site within the ion channel, which was photolabeled in the resting, closed channel state (–agonist) but not in the desensitized state (+agonist), and (ii) an intrasubunit site within the δ subunit helix bundle, homologous to the propofol binding site in GLIC, which was photolabeled in the nAChR desensitized state (+agonist) but not in the resting state. The inhibition of ion-channel photolabeling may be allosteric because propofol desensitizes the *Torpedo* nAChR in the absence of agonist. In the presence of agonist, however, propofol inhibition of photolabeling in the δ subunit helix-bundle pocket ($\delta\text{Phe-232}$ and $\delta\text{Cys-236}$ (M1) and $\delta\text{Thr-274}$ (M2), Figure 4E) appears competitive, indicating that both propofol (volume, 180 Å³) as well as AziPm (volume, 178 Å³) bind in the desensitized state to this intrasubunit site. Photoaffinity-labeling studies have established that this pocket within the δ subunit helix bundle is a binding site for other small, hydrophobic nAChR inhibitors, including the volatile general anesthetic [^{14}C]halothane (volume, 85 Å³)³³ and a drug related in structure to AziPm,

[^{125}I]TID (3-(trifluoromethyl)-3-(*m*-iodophenyl)diazirine (volume, 150 Å³). Similar to AziPm, [^{125}I]TID photolabeled this site in the equilibrium desensitized state but not in the resting state.³⁴ Although GLIC and *Torpedo* nAChR have an intrasubunit helix-bundle binding site for small hydrophobic inhibitors in common, the site in GLIC is located predominantly between the M1, M3, and M4 helices, whereas the site in the nAChR is between the M1, M2, and M3 helices (Figure 4D,E).

We also found evidence of [^3H]AziPm photolabeling at a lower efficiency for amino acids in M3 (Tyr-263 and Tyr-266) that contribute to the pocket at the interface between subunits, but this photolabeling was not inhibited by propofol at 300 μM . Thus, we found no evidence in our photolabeling study that propofol binds to an intersubunit site in GLIC in detergent at pH 4.4 equivalent to the intersubunit GLIC propofol binding site predicted on the basis of propofol's protection at pH 8 of modification of the GLIC L241C mutant expressed in *Xenopus* oocytes.¹⁴ Because, in that study, it was also shown that propofol enhanced the rate of modification of a Cys substituted for Thr-255, which projects within the intrasubunit propofol binding pocket in the crystal structure adjacent to our photolabeled Tyr-254 in M3 (Figure 4D), further studies are required to determine whether propofol binds preferentially in GLIC in detergent to an intrasubunit site at pH 4.4 (open/desensitized states) but to an intersubunit site at pH 8 (resting, closed channel state). Strong state dependence has been seen for drug binding to the homologous intrasubunit binding site in the δ subunit of the *Torpedo* nAChR in native membranes, which was not photolabeled by [^{125}I]TID in the resting state and was photolabeled in the transient open/fast desensitized states at >20 -fold higher efficiency than in the equilibrium desensitized state.^{27,35} However, recent electron spin resonance studies found evidence of a pH-dependent change in the structure of purified GLIC reincorporated into liposomes but not in detergent solution.³⁶

Although propofol and AziPm, inhibitors of GLIC and the nAChR, bind to equivalent intrasubunit binding sites in these pLGICs, these anesthetics are unlikely to bind to equivalent sites in GABA_ARs when they potentiate GABA responses. On the basis of the locations in early GABA_AR structural models of the GABA_AR amino acids in the β -subunit M1 and M3 helices that were identified by mutational analyses as propofol- and etomidate-sensitivity determinants, these anesthetics were proposed to bind to an intrasubunit site within the β subunit that would be analogous to the propofol binding site in GLIC (reviewed in ref 37). However, in more robust GABA_AR structural models that can now be derived from the structures of GLIC or GluCl, these β -subunit anesthetic-sensitivity determinants are located within an intersubunit binding site at the interface between the β and α subunits.^{17,38} Identification of GABA_AR general anesthetic binding sites by use of photoreactive etomidate and barbiturate analogues has established that there are two classes of intersubunit anesthetic binding sites in the $\alpha\beta\gamma$ GABA_AR transmembrane domain: one at the $\beta^+-\alpha^-$ subunit interfaces that contain the GABA binding site in the extracellular domain and the second at the $\alpha^+-\beta^-$ and $\gamma^+-\beta^-$ interfaces.^{16,18} Although etomidate binds selectively to the $\beta^+-\alpha^-$ sites and some barbiturates bind selectively to the $\alpha^+/\gamma^+-\beta^-$ sites, propofol binds to both sites with similar affinity on the basis of the concentration dependence of propofol inhibition of photolabeling.¹⁸ Direct photolabeling of GABA_ARs with [^3H]AziPm or other recently developed photoreactive

propofol analogues^{39,40} will be necessary to determine whether propofol also binds to intrasubunit sites in GABA_AR equivalent to the propofol site in GLIC.

■ ASSOCIATED CONTENT

■ Supporting Information

Stereo images of pLGIC subunit domains showing the structures of GLIC (PDB: 3P50) and the nAChR δ subunit in a GLIC-derived homology model compared with the nAChR cryoelectron microscopy structure (PDB: 2BG9). Representative distances between photolabeled residues in the two nAChR structures. This material is available free of charge via the Internet at <http://pubs.acs.org>.

■ AUTHOR INFORMATION

Corresponding Authors

*(P.T.) E-mail: tangp@upmc.edu. Phone: (412) 383-9798.

*(J.B.C.) E-mail: Jonathan_Cohen@hms.harvard.edu. Phone: (617) 432-1728.

Funding

This research was supported in part by USPHS grants GM-06358 (P.T.), GM-58448 (J.B.C.), and GM-55876 (R.G.E.).

Notes

The authors declare no competing financial interest.

■ ABBREVIATION USED

pLGIC, pentameric ligand-gated ion channel; GLIC, *Gloeobacter violaceus* ligand-gated ion channel; AziPm, 2-isopropyl-5-[3-(trifluoromethyl)-3H-diazirin-3-yl]phenol; nAChR, nicotinic acetylcholine receptor; GABA_AR, γ -aminobutyric acid type-A receptor; PPF, propofol; OPA, o-phthalaldehyde; EndoLys-C, *Lysobacter enzymogenes* endoprotease Lys-C; TMD, transmembrane domain

■ REFERENCES

- (1) Krasowski, M. D.; Jenkins, A.; Flood, P.; Kung, A. Y.; Hopfinger, A. J.; and Harrison, N. L. (2001) General anesthetic potencies of a series of propofol analogs correlate with potency for potentiation of gamma-aminobutyric acid (GABA) current at the GABA(A) receptor but not with lipid solubility. *J. Pharmacol. Exp. Ther.* 297, 338–351.
- (2) Rudolph, U., and Antkowiak, B. (2004) Molecular and neuronal substrates for general anaesthetics. *Nat. Rev. Neurosci.* 5, 709–720.
- (3) Franks, N. P. (2008) General anaesthesia: From molecular targets to neuronal pathways of sleep and arousal. *Nat. Rev. Neurosci.* 9, 370–386.
- (4) Dilger, J. P.; Vidal, A. M.; Mody, H. I.; and Liu, Y. (1994) Evidence for direct actions of general anesthetics on an ion channel protein. A new look at a unified mechanism of action. *Anesthesiology* 81, 431–442.
- (5) Violet, J. M.; Downie, D. L.; Nakisa, R. C.; Lieb, W. R.; and Franks, N. P. (1997) Differential sensitivities of mammalian neuronal and muscle nicotinic acetylcholine receptors to general anesthetics. *Anesthesiology* 86, 866–874.
- (6) Flood, P.; Ramirezlatorre, J.; and Role, L. (1997) $\alpha 4\beta 2$ neuronal nicotinic acetylcholine receptors in the central nervous system are inhibited by isoflurane and propofol, but $\alpha 7$ -type nicotinic acetylcholine receptors are unaffected. *Anesthesiology* 86, 859–865.
- (7) Weng, Y.; Yang, L. Y.; Corringer, P. J.; and Sonner, J. M. (2010) Anesthetic sensitivity of the *Gloeobacter violaceus* proton-gated ion channel. *Anesth. Analg.* 110, 59–63.
- (8) Unwin, N. (2005) Refined structure of the nicotinic acetylcholine receptor at 4 Å resolution. *J. Mol. Biol.* 346, 967–989.
- (9) Baenziger, J. E., and Corringer, P. J. (2011) 3D structure and allosteric modulation of the transmembrane domain of pentameric ligand-gated ion channels. *Neuropharmacology* 60, 116–125.

- (10) Nury, H.; Van Renterghem, C.; Weng, Y.; Tran, A.; Baaden, M.; Dufresne, V.; Changeux, J. P.; Sonner, J. M.; Delarue, M.; and Corringer, P. J. (2011) X-ray structures of general anaesthetics bound to a pentameric ligand-gated ion channel. *Nature* 469, 428–431.
- (11) Sauguet, L.; Howard, R. J.; Malherbe, L.; Lee, U. S.; Corringer, P. J.; Adron Harris, R.; and Delarue, M. (2013) Structural basis for potentiation by alcohols and anaesthetics in a ligand-gated ion channel. *Nat. Commun.* 4, 1697.
- (12) Pan, J. J.; Chen, Q.; Willenbring, D.; Mowrey, D.; Kong, X. P.; Cohen, A.; Divito, C. B.; Xu, Y.; and Tang, P. (2012) Structure of the pentameric ligand-gated ion channel GLIC bound with anesthetic ketamine. *Structure* 20, 1463–1469.
- (13) Spurny, R.; Billen, B.; Howard, R. J.; Brams, M.; Debaveye, S.; Price, K. L.; Weston, D. A.; Strelkov, S. V.; Tytgat, J.; Bertrand, S.; Bertrand, D.; Lummis, S. C. R.; and Ulens, C. (2013) Multisite binding of a general anesthetic to the prokaryotic pentameric *Erwinia chrysanthemi* ligand-gated ion channel (ELIC). *J. Biol. Chem.* 288, 8355–8364.
- (14) Ghosh, B.; Satyshur, K. A.; and Czajkowski, C. (2013) Propofol binding to the resting state of the *Gloeobacter violaceus* ligand-gated ion channel (GLIC) induces structural changes in the inter- and intrasubunit transmembrane domain (TMD) cavities. *J. Biol. Chem.* 288, 17420–17431.
- (15) Vodovozova, E. L. (2007) Photoaffinity labeling and its application in structural biology. *Biochemistry (Moscow)* 72, 1–20.
- (16) Li, G.-D.; Chiara, D. C.; Sawyer, G. W.; Husain, S. S.; Olsen, R. W.; and Cohen, J. B. (2006) Identification of a GABAA receptor anesthetic binding site at subunit interfaces by photolabeling with an etomidate analog. *J. Neurosci.* 26, 11599–11605.
- (17) Chiara, D. C.; Dostalova, Z.; Jayakar, S. S.; Zhou, X.; Miller, K. W.; and Cohen, J. B. (2012) Mapping general anesthetic binding site(s) in human $\alpha 1\beta 3 \gamma$ -aminobutyric acid type A receptors with [³H]TDBzl-etomidate, a photoreactive etomidate analogue. *Biochemistry* 51, 836–847.
- (18) Chiara, D. C.; Jayakar, S. S.; Zhou, X.; Zhang, X.; Savechenkov, P. Y.; Bruzik, K. S.; Miller, K. W.; and Cohen, J. B. (2013) Specificity of intersubunit general anesthetic-binding sites in the transmembrane domain of the human $\alpha 1\beta 3\gamma 2$ γ -aminobutyric acid type A (GABAA) receptor. *J. Biol. Chem.* 288, 19343–19357.
- (19) Hall, M. A.; Xi, J.; Lor, C.; Dai, S.; Pearce, R.; Dailey, W. P.; and Eckenhoof, R. G. (2010) m-Azipropofol (AziPm) a photoactive analogue of the intravenous general anesthetic propofol. *J. Med. Chem.* 53, 5667–5675.
- (20) Jayakar, S. S.; Dailey, W. P.; Eckenhoof, R. G.; and Cohen, J. B. (2013) Identification of propofol binding sites in a nicotinic acetylcholine receptor with a photoreactive propofol analog. *J. Biol. Chem.* 288, 6178–6189.
- (21) Bocquet, N.; de Carvalho, L. P.; Cartaud, J.; Neyton, J.; Le Poupon, C.; Taly, A.; Grutter, T.; Changeux, J.-P.; and Corringer, P.-J. (2007) A prokaryotic proton-gated ion channel from the nicotinic acetylcholine receptor family. *Nature* 445, 116–119.
- (22) Chen, Q.; Cheng, M. H.; Xu, Y.; and Tang, P. (2010) Anesthetic binding in a pentameric ligand-gated ion channel: GLIC. *Biophys. J.* 99, 1801–1809.
- (23) Crimmins, D. L.; McCourt, D. W.; Thoma, R. S.; Scott, M. G.; Macke, K.; and Schwartz, B. D. (1990) In situ chemical cleavage of proteins immobilized to glass-fiber and polyvinylidene difluoride membranes: Cleavage at tryptophan residues with 2-(2'-nitrophenylsulfenyl)-3-methyl-3'-bromoindolenine to obtain internal amino acid sequence. *Anal. Biochem.* 187, 27–38.
- (24) Brauer, A. W.; Oman, C. L.; and Margolies, M. N. (1984) Use of o-phthalaldehyde to reduce background during automated Edman degradation. *Anal. Biochem.* 137, 134–142.
- (25) Middleton, R. E.; and Cohen, J. B. (1991) Mapping of the acetylcholine binding site of the nicotinic acetylcholine receptor: [³H]-Nicotine as an agonist photoaffinity label. *Biochemistry* 30, 6987–6997.
- (26) Bondarenko, V.; Mowrey, D.; Tillman, T.; Cui, T.; Liu, L. T.; Xu, Y.; and Tang, P. (2012) NMR structures of the transmembrane

domains of the $\alpha 4\beta 2$ nAChR. *Biochim. Biophys. Acta* 1818, 1261–1268.

(27) Arevalo, E., Chiara, D. C., Forman, S. A., Cohen, J. B., and Miller, K. W. (2005) Gating-enhanced accessibility of hydrophobic sites within the transmembrane region of the nicotinic acetylcholine receptor's δ -subunit. A time-resolved photolabeling study. *J. Biol. Chem.* 280, 13631–13640.

(28) Garcia, G. I., Chiara, D. C., Nirthanan, S., Hamouda, A. K., Stewart, D. S., and Cohen, J. B. (2007) [^3H]Benzophenone photolabeling identifies state-dependent changes in nicotinic acetylcholine receptor structure. *Biochemistry* 46, 10296–10307.

(29) Hamouda, A. K., Stewart, D. S., Husain, S. S., and Cohen, J. B. (2011) Multiple transmembrane binding sites for p-trifluoromethyl-diaziriny-*etomidate*, a photoreactive *Torpedo* nicotinic acetylcholine receptor allosteric inhibitor. *J. Biol. Chem.* 286, 20466–20477.

(30) Velisetty, P., and Chakrapani, S. (2012) Desensitization mechanism in prokaryotic ligand-gated ion channel. *J. Biol. Chem.* 287, 18467–18477.

(31) Velisetty, P., Chalamalasetti, S. V., and Chakrapani, S. (2012) Conformational transitions underlying pore opening and desensitization in membrane-embedded *Gloeobacter violaceus* ligand-gated ion channel (GLIC). *J. Biol. Chem.* 287, 36864–36872.

(32) Mowrey, D., Cheng, M. H., Liu, L. T., Willenbring, D., Lu, X. H., Wymore, T., Xu, Y., and Tang, P. (2013) Asymmetric ligand binding facilitates conformational transitions in pentameric ligand-gated ion channels. *J. Am. Chem. Soc.* 135, 2172–2180.

(33) Chiara, D. C., Dangott, L. J., Eckenhoff, R. G., and Cohen, J. B. (2003) Identification of nicotinic acetylcholine receptor amino acids photolabeled by the volatile anesthetic halothane. *Biochemistry* 42, 13457–13467.

(34) Hamouda, A. K., Chiara, D. C., Blanton, M. P., and Cohen, J. B. (2008) Probing the structure of the affinity-purified and lipid-reconstituted *Torpedo* nicotinic acetylcholine receptor. *Biochemistry* 47, 12787–12794.

(35) Yamodo, I. H., Chiara, D. C., Cohen, J. B., and Miller, K. W. (2010) Conformational changes in the nicotinic acetylcholine receptor during gating and desensitization. *Biochemistry* 49, 156–165.

(36) Dellisanti, C. D., Ghosh, B., Hanson, S. M., Raspanti, J. M., Grant, V. A., Diarra, G. M., Schuh, A. M., Satyshur, K., Klug, C. S., and Czajkowski, C. (2013) Site-directed spin labeling reveals pentameric ligand-gated ion channel gating motions. *PLoS Biol.* 11, e1001714–1–e1001714-14.

(37) Hemmings, H. C., Akabas, M. H., Goldstein, P. A., Trudell, J. R., Orser, B. A., and Harrison, N. L. (2005) Emerging molecular mechanisms of general anesthetic action. *Trends Pharmacol. Sci.* 26, 503–510.

(38) Bertaccini, E. J., Yoluk, O., Lindahl, E. R., and Trudell, J. R. (2013) Assessment of homology templates and an anesthetic binding site within the γ -aminobutyric acid receptor. *Anesthesiology* 119, 1087–1095.

(39) Stewart, D. S., Savechenkov, P. Y., Dostalova, Chiara, D. C., Ge, R., Raines, D. E., Cohen, J. B., Forman, S. A., Bruzik, K. S., and Miller, K. W. (2011) p-(4-Azipentyl)propofol: A potent photoreactive general anesthetic derivative of propofol. *J. Med. Chem.* 54, 8124–8135.

(40) Yip, G. M. S., Chen, Z. W., Edge, C. J., Smith, E. H., Dickinson, R., Hohenester, E., Townsend, R. R., Fuchs, K., Sieghart, W., Evers, A. S., and Franks, N. P. (2013) A propofol binding site on mammalian GABAA receptors identified by photolabeling. *Nat. Chem. Biol.* 9, 715–720.

(41) Chiara, D. C., Hong, F. H., Arevalo, E., Husain, S. S., Miller, K. W., Forman, S. A., and Cohen, J. B. (2009) Time-resolved photolabeling of the nicotinic acetylcholine receptor by [^3H]-azietomidate, an open-state inhibitor. *Mol. Pharmacol.* 75, 1084–1095.